RJC

RASĀYAN *J. Chem.*
Vol. 15 | No. 1 |57-64| January - March | 2022
ISSN: 0974-1496 | e-ISSN: 0976-0083 | CODEN: RJCABP
http://www.rasayanjournal.com
http://www.rasayanjournal.co.in

SYNERGISTIC CORROSION-WEAR EFFECT IN AUSTENITIC POWDER METALLURGICAL STEEL WITH DIFFERENT TITANIUM ADDITIONS

W. Aperador[1,✉], J. Bautista-Ruiz[2] and J. Caicedo[3]

[1]Universidad ECCI, Bogotá-111156, Colombia

[2]Engineering Faculty, Universidad Francisco de Paula Santander, San José de Cúcuta-540005, Colombia

[3] Department of Physics, Universidad del Valle, Cali-760034, Colombia

✉Corresponding author: g.ing.materiales@gmail.com

ABSTRACT

To ascertain the influence of titanium percentage in 316L austenitic steel, titanium percentages varied from 0.5 to 2% aggregated to 316L steel. The powder metallurgy method was used. The powdered material was pressed at 800 MPa and then sintered at 1300°C. The X-ray diffraction (XRD) technique was used to characterize the identification of the phases after the processed mixtures. Wear and tribowear properties were determined by pin on disc tests. Electrochemical polarization curves were used to study corrosion. According to the results of the samples, the corrosion resistance of titanium increased to a percentage of 1.5% due to the formation of the phases generated by the mixture. However, it was determined that the most appropriate percentage is 2%, due to the synergistic mode specifically for wear and corrosion resistance, the mechanism is the most adequate.

Keywords: 316L Steel, Titanium, Corrosion, Powder Metallurgy, Tribology.

RASĀYAN *J. Chem.*, Vol. 15, No.1, 2022

INTRODUCTION

The powder metallurgy production method consists principally of four phases, which are as follows: Determination of the base powder, mixing, pressing and sintering.[1] Powder metallurgy is a unique mixture of materials with dissimilar or extremely high melting points that tend to react abruptly with the environment when melted. The chemical classification of metallic powders can be divided into elemental and pre-alloyed.[2] Elemental powders are made of pure metal and are used for applications where high purity is important, in this study, titanium was used; however, the more common are iron, aluminum and copper.[3] In pre-alloyed powders, each particle is an alloy that has the desired chemical composition, these are used when the alloy cannot be manufactured by mixing elemental powders, the most commonly used is stainless steel.[4] Obtaining these characteristics involves mixing powders of different sizes and compositions until a homogenous mixture of all components is attained. Some additives are added as lubricants during compaction or binders to increase the compaction strength.[5] Blended powders are compressed by mechanical or hydraulic pressure in a matrix, by means of compaction, it is possible to obtain pieces with precise dimensions and finishes, resulting in high productivity in the industry by means of this technique. In the sintering process, the toughness is acquired to perform the engineering function for which it has been manufactured.[6] It consists essentially of heat treatment at a temperature lower than the melting temperature of the principal component (1400°C) in the case of 316L steel.

Austenitic steel 316L is referred to as stainless steel since it resists corrosion more than other steels; however, it is susceptible to pitting corrosion.[7] However, stainless steel implants that are produced by the powder metallurgy technique may improve the mechanical properties, since they can be designed according to the grain size, additionally, homogeneity of the material is provided, and allow the production of final size and high quality implants that can be cost-effective, and it is possible to avoid defects of the material, and also to improve the quality and homogeneity of the material, and allow the manufacturing of final size and high quality implants that can be cost-effective, and it is feasible to avoid potential defects of the

http://dx.doi.org/10.31788/RJC.2022.1516622

material, and it is also possible to produce high quality implants that can be cost-effective, and it is possible to avoid possible defects of the material, since they can be designed according to the grain size, additionally homogeneity of the material is obtained, and they allow the production of implants of final size and high quality that can be profitable, in addition it is possible to avoid possible casting defects.[8,9]
The aim of this article is to obtain materials that can resist suitable conditions that can be used in dentistry and that these materials generate the highest possible service life, analyzing the effect of mechanical alloying in pure austenitic steel concerning titanium concentrations of 0.5%, 1%, 1.5% and 2%, obtaining metallic matrix and establishing the interrelationship between the tribological behavior and corrosion resistance of the samples, the results indicated that it is possible to achieve an industrial application.

EXPERIMENTAL

In sample fabrication, a process conditioning analysis was developed related to the compaction of the powders before and after sintering. AISI 316L powders with a chemical composition of Cr 18.2%, Ni 13.2%, Mo 2.9%, Mn 0.32%, Si 0.8%, C 0.092 % and the rest Fe were used for the conditioning process, with a specific mass of 7.09 g/cm^3. Titanium powders were 99.9% pure and were added to the stainless-steel powders in mass percentages of 0.5%, 1%, 1.5% and 2%. Zn-Sterat (0.6%) was added into the powder as a lubricant. A total of 4 groups of samples were obtained. The mixing process was carried out in a conical mixer at 30 rpm for 60 minutes. The powders were compacted by uniaxial compression at a rate of 0.5mm/s and a load of 8157.73 kgf/cm² using an INSTRON model 4507 mold and universal testing machine. Afterward, the samples were sintered, beginning with a heating ramp up to 500 °C in 60 minutes. For 30 minutes at 500 °C. The temperature is then raised to 1300°C for 60 minutes and maintained at this temperature for 40 minutes. In the cooling process, it is reduced to 910 °C in the oven. Morphological characterization was performed using the scanning electron microscopy technique on a Jeol JSM6490LV. The collected pictures provided information concerning the morphology and dimensions of the particles. Mineralogical and structural characterizations of the samples were performed by X-ray diffraction using a Bruker D8 Advance A25 diffractometer with Co-Kα monochromatic radiation with a wavelength of 1.78900 Å, Bragg-Brentano geometry, goniometer in θ/θ configuration, scanning range 2θ between 10° and 90°, and step of 0.02° and 2 seconds. The analysis focused on identifying the crystalline phases present in the materials studied with the related spectra in the database (Crystallography Open Database).
Additionally, the parameters involved were adjusted from the refinement until the difference between the theoretical and the experimental diffraction pattern became minimal. Damage caused by the corrosive fluid was determined by means of potentiodynamic polarization curves with a Princeton Applied Research potentiostat - galvanostat, model Versastat II. A three-electrode electrochemical cell was used: Ag/AgCl reference electrode, counter electrode (platinum wire) and the compacted material as working electrode. The contact area of the sample was 1 cm^2. The electrodes were immersed in a solution that simulates human saliva conditions, whose composition is: urea (1 g/l), $NaH_2PO_4 \bullet 2H_2O$ (0.690 g/l), $Na_2S_9H_2O$ (0.005 g/l), $CaCl_2 \bullet 2H_2O$ (0.906 g/l), KCl (0.4 g/l) and NaCl (0.4 g/l), the pH of the solution was 6.4, Electrodes are immersed in a solution that simulates saliva conditions and since corrosion of metallic implants is of vital importance because it can negatively affect the biocompatibility and mechanical integrity of the implants as well as corroding active metals by forming chlorides on the metal. The potentiodynamic polarization curves were obtained at a sweep speed of 0.125 mV/s, the voltage range of -0.25 V to 0.25 V and the evaluation area of 1 cm^2. On a pin on disk equipment, specimens were used with a flat shaft and a rotational speed of 50 m/min at a constant rate. The tribological pair used in the study corresponded to a bone pin and the samples obtained by powder metallurgy. The tests were carried out at a temperature of 37 °C. Tribocorrosion tests were carried out using a High-Temperature Tribometer: THT :: Anton-Paar, at a temperature of 37 °C (Normal body temperature) in order to study the influence of the synergy between abrasive wear and corrosion. To the tribometer was adapted an electrochemical cell composed of a series of three electrodes, the reference electrode (Ag/AgCl), the counter electrode (platinum wire) and the working electrode located in the sample holder with an exposure area of the specimen of 1 cm^2 and containing the electrolyte. A potentiostat - galvanostat was used to evaluate corrosion and wear resistance, with the same specifications as previously mentioned in the corrosion study.

RESULTS AND DISCUSSION

Figure-1 is the spectrum where the crystal structure evolution was determined in the 4 studied systems varying the titanium concentrations: 316L+0.5%Ti, 316L+1%Ti, 316L+1.5%Ti and 316L+2%Ti.[10] The X-ray diffraction results indicated polycrystallinity of the samples showing preferential growths in the crystallographic directions (111) at 44.48°, (100) at 43.5°, (020) at 52.14°, (101) at 50.84°, and (102) at 68.12°.[11] The materials studied revealed face-centered cubic (FCC) crystal structure with lattice parameters a=b=c=3.49 Å, α= β=ɣ=90°, the density of 8.7 g/cm^3 and cell volume of 42.65x106 pm^3. In the diffraction pattern of 316L +2%Ti (red spectrum) Ti is represented by the crystallographic directions where the peak with the highest intensity is observed (011) at 38.2° and (022) at 2θ~76. 43° corresponding to the face-centered cubic structure with space group IM- 3m, with parameters a=b=c=3.18 Å, α= β=ɣ=90°, with a density of 5.11 g/cm^3 and a cell volume of 32.16x106 pm^3. An increase of the signals in the diffractograms is observed in the materials with Titanium content, which is explained due to the increase of the Fe-Ti phase, in the formation of powder metallurgical materials, this increase can generate improvements in the mechanical and tribological properties due to the high density of the crystalline structure.[12,13] With increasing Ti content to a value close to 2 %, the percentage of titanium allows a reduction of porosity at the grain boundaries due to the metallic bonding generated.

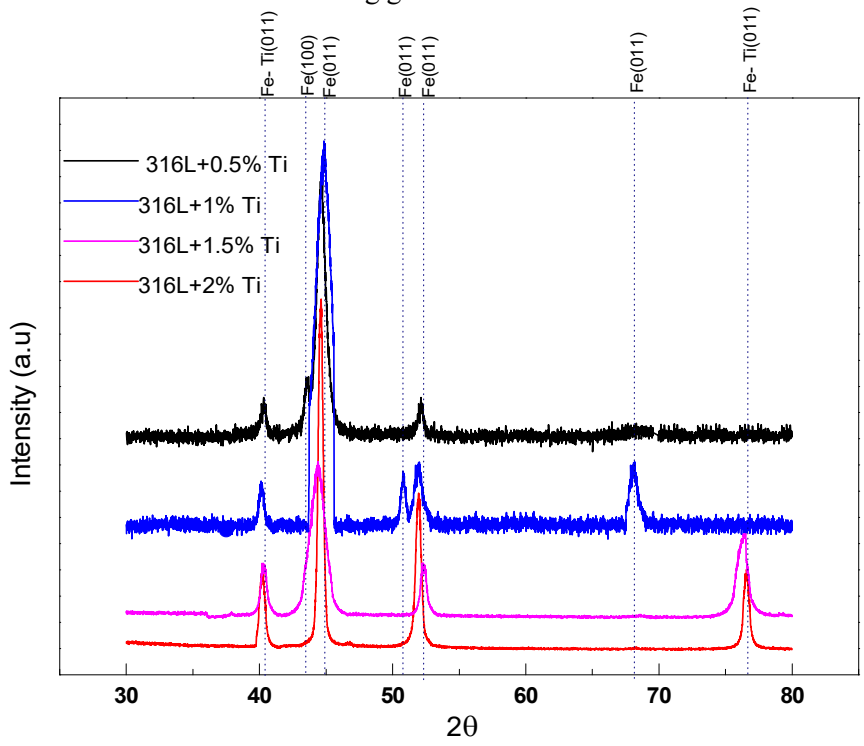

Fig.-1: X-ray Diffraction Spectra Corresponding to the Alloyed Specimens with Different Percentages of Titanium with Variations from 0.5% to 2%.

Figure-2 demonstrates the corrosion behavior of the materials under study by means of potentiodynamic polarization curves using the salivary solution and 37°C temperature conditions.[14] From the polarisation potentiodynamic curves, the corrosion current intensity, corrosion potential and corrosion rate were determined for powder metallurgy materials at different titanium concentrations (0.5%, 1%, 1.5% and 2%).[15] The information related to the above parameters is registered in Table-1. With regard to steel with the addition of 2% Titanium (316L+2%Ti), Fig.-2 demonstrates the typical behavior for stainless steel.[16,17] The curve evidence, at negative potentials, a general dissolution zone and more positive potentials, it reaches the pitting zone. It is characterized by an increase in current at constant potentials in this region, which causes pitting corrosion phenomena and is caused by the protective oxide layer on the surface of the steel being fractured.[18]

This fracture permits the metal to become susceptible to electron loss. In the samples with Ti content lower than 2% (316L+0.5%Ti, 316L+1%Ti, and 316L+1.5%Ti), a significantly improved electrochemical performance was evidenced.[19] This is explained by the fact that the positive potential for the three curves indicated a general dissolution and in the polarization curves, the corrosion currents are high when analyzed at a constant potential. Nevertheless, the 316L+2%Ti sample indicated a reduced corrosion current density in comparison to the other alloys analyzed.[20]

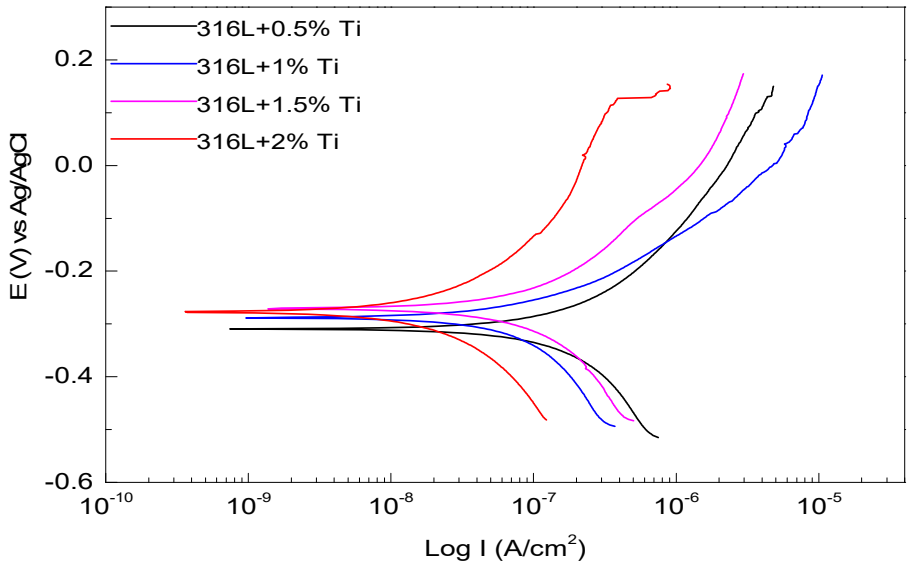

Fig.-2: Potentiodynamic Polarisation Curves of Titanium Combinations with Steel

Table-1 provides the corrosion parameters obtained from the potentiodynamic polarization curves of the samples analyzed. It is possible to analyze from the results that the addition of titanium powders to 316L steel improved the anti-corrosion response of the steel-titanium composite when subjected to environments with the presence of chlorides, as in the case of the salivary environment.[19] This behavior is probably attributed to the conformation of the stainless steel's own protective layer. Considering the above, it was corroborated that the samples with higher percentages of titanium in them presented the highest anti-corrosion conditions, as can be seen in figure 2. These behaviors can be explained by the propensity of the material to form higher crystallinity as the titanium addition increases, as observed in figure 1. In addition, the growth of finer grains tends to generate high levels of free energy at the grain boundaries. Therefore, a system with low titanium content is more susceptible to pitting corrosion damage when in a highly corrosive environment.

Table-1: Parameters Obtained from the Potentiodynamic Polarisation Curves

	E_{corr} *(mV vs Ag/AgCl)*	I_{corr} *(A/cm²)*	V_{corr} *(µm/y)*
316L+0.5%	-0.31	0.921	6.1214
316L+1%	-0.28	0.559	3.7084
316L+1.5%	-0.27	0.520	3.4544
316L+2%	-0.27	0.114	0.7366

Figure-3 indicates the tribological performance for the materials obtained at different titanium concentrations. Tribological performance was measured using a bone pin in contact with the sample specimens.[21] This provides information regarding the coefficient of friction and wear. The coefficient of friction curves generally starts with the start-up phase influenced by static friction followed by dynamic friction (where high friction and wear are found), the sliding surfaces are partially separated due to the lubricating film (the solution used for the simulation). For the 316L+0.5%Ti and 316L+1%Ti materials, the distance required to arrive at the wear condition was 14m. In the 316L+1.5%Ti and 316L+2%Ti systems,

the friction coefficient of friction was low up to 40m and then increased, being more notorious for the 316L+1.5%Ti system.[22] From the study, it was concluded that the behavior of the analyzed systems indicated different wear mechanisms as abrasive types.

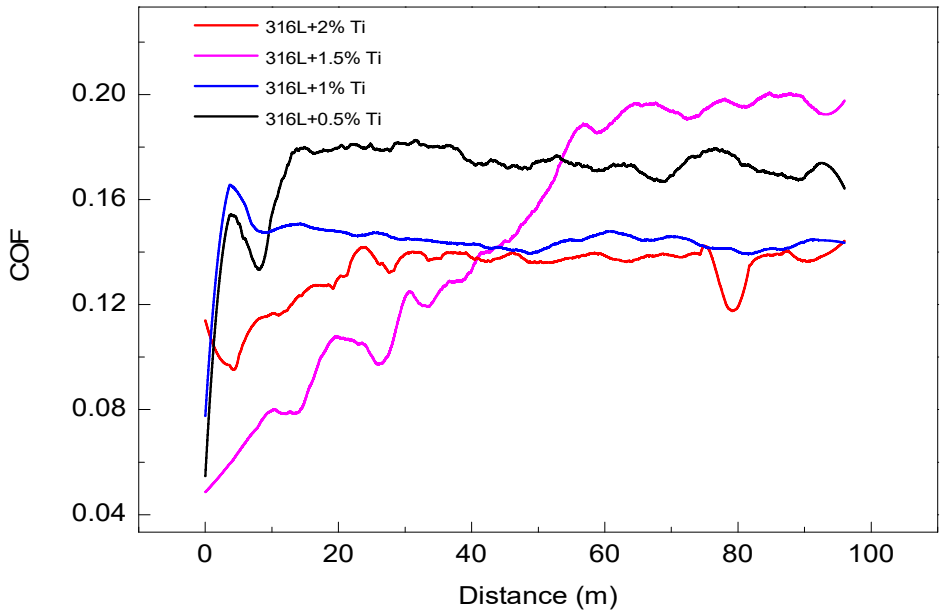

Fig.-3: Coefficient of Friction for 316L+0.5%Ti, 316L+1%Ti, 316L+1.5%Ti and 316L+2%Ti Combinations

Figure-4 provides the micrographs obtained by the scanning electron microscopy technique. This analysis consisted of comparing the samples before and after the corrosion-assisted wear deterioration tests. Figure-4a indicates a micrograph for the 316L+0.5%Ti system in which the phenomenon of abrasive wear predominates, generating grooves on the surface. As the grooves are not present on the entire surface, it can be assumed that the surface wear is produced by abrasive particles since the working fluid removed the less adhered layer and recirculated in the system, creating areas of increased wear. For the 316L+1Ti system (Fig.-4b), the raceways are of smaller diameter as compared to Fig.-4a, although it can be depicted by the same wear mechanisms as the 316L+0.5Ti system. Therefore, the wear rate is lower.[23] The value of the coefficient of friction for this 316L+0.5Ti system was determined to be 0.14 (Fig.-3). In contrast, the coefficient of friction for the 316L+1Ti system was 0.18, in this case, the passive film is a protective layer and avoids the formation of abrasive particles. The micrograph for the 316L+1.5Ti system revealed evidence of greater wear compared to the results for the 316L+1Ti system. When correlating the 316L+1.5Ti and 316L+0.5Ti, respectively, shallow raceways were indicated for the latter. This type of behavior was related to a third body that affects the fracture toughness due to the stress distribution in the material that had a Titanium content higher than 1.5%. The above described can be indicated in Fig.-4c in the micrograph obtained after the test and where the wear tracks in these materials are thin and parallel to the sliding movement of the pin. This type of behavior was related to a third body that affects the fracture toughness due to the stress distribution in the material that had a Titanium content higher than 1.5%. The previously reported can be indicated in Fig.-4c in the micrograph after testing and where the wear paths in these materials are thin and parallel to the sliding movement of the pin.[24] These characteristics suggest that abrasion is the main wear mechanism and coincides with the wear mechanisms proposed for this type of material.

Additionally, it was determined from the coefficient of friction plots that the origin of the wear type was adhesive since it initiated at about 0.04. It was concluded, to some extent, that a greater amount of wear particles is generated, which impact an interface zone between the pin and the specimen. Additionally, the working solution increased the amount of wear particles and generated recirculation of abrasive particles.

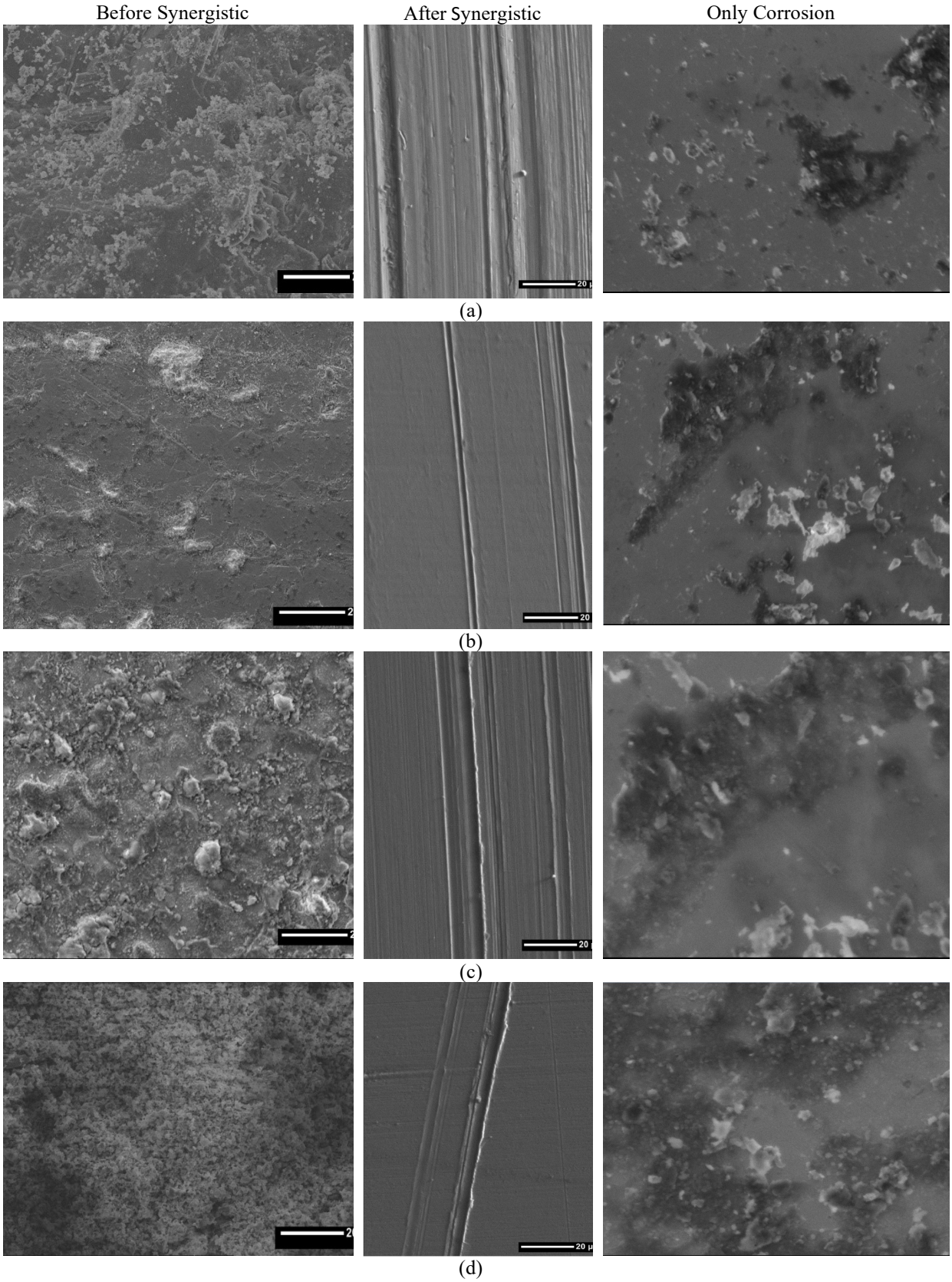

Fig.-4: Before and after Synergistic Test Micrographs and Corrosion Tests (a)316L+0.5%Ti, (b) 316L+1%Ti, (c) 316L+1.5%Ti and (d) 316L+2%Ti.

For the 316L+2Ti system (Fig.-4d) a surface with reduced wear raceways due to higher concentrations of titanium in the material improving adhesion was then indicated. It is important to highlight that less dissolution and a lower corrosion rate were indicated in the results obtained in the potentiodynamic polarization curves for the 316L+2Ti system.[25] However, the pitting corrosion phenomenon occurred with the breakage of the protective oxide film and continued with the formation of surface fissures. This behaviour was related to the decrease in the friction coefficient at around 80 m and its subsequent increase, generating values close to those found for the 316L+1.5Ti system.

CONCLUSION

Titanium concentration has an impact on each of the results obtained. In the performance of the different properties and especially the corrosion wear synergy, with respect to the corrosion resistance by the electrochemical method according to the potentiodynamic polarization curves, the 316L steel with the addition of titanium exhibits lower corrosion rates as the amount of titanium increases.

The corrosion performance is not the most adequate, as a percentage of 2% shows pitting corrosion.

The corrosion resistance and tribological performance of the coatings are different in response to the amount of titanium and are related to the microstructural behaviour and morphology, 316 steels with a higher addition of titanium have a reduced wear coefficient compared to the 0.5%, 1% and 1.5% titanium additions.

In general, 316 steels with the addition of titanium improve in all the tests evaluated, this is due to the fact that the passive layer enhances the properties of the steel.

REFERENCES

1. H. Kulkarni and V.V. Dabhade, *Journal of Manufacturing Processes*, **44**, 1(2019), https://doi.org/10.1016/j.jmapro.2019.05.009
2. A. Billard, F. Maury, P. Aubry, F. Balbaud-Célérier, B. Bernard, F. Lomello, H. Maskrot, E. Meillot, A. Michau and F. Schuster, *Comptes Rendus Physique*, **19(8)**, 755(2018), https://doi.org/10.1016/j.crhy.2018.10.005
3. J. Caicedo, N. Bonilla, W. Aperador, *Metals*, **11(12)**, 11122049 (2021), https://doi.org/10.3390/met11122049
4. A. Kumar-Rai, S. Raju, B. Jeya Ganesh, G. Panneerselvam, M. Vijayalakshmi, T. Jayakumar and B. Raj, *Nuclear Engineering and Design*, **241(8)**, 2787(2011), https://doi.org/10.1016/j.nucengdes.2011.05.039
5. U. Pandey, R. Purohit, P. Agarwal and S. Kumar Singh, *Materials Today: Proceedings*, **5(2)**, 4106(2018), https://doi.org/10.1016/j.matpr.2017.11.671
6. N. Zhang, X. Han, D. Sun, S. Liu, H. Liu, W. Yang and G. Wu, *Powder Technology*, **369**, 334(2020), https://doi.org/10.1016/j.powtec.2020.05.030
7. N. Karthikeyan, B. Radha Krishnan, A. VembathuRajesh and V. Vijayan, *Materials Today: Proceedings*, **37(2),** 2770(2021), https://doi.org/10.1016/j.matpr.2020.08.643
8. N. Akçaml and B. Şenyurt, *Ceramics International*, **47(5)**, 6813(2021), https://doi.org/10.1016/j.ceramint.2020.11.024
9. D. Yang, S. Guo, J. Chen, C. Qiu, S. Oshioke - Agbedor, A. Ma, J. Jiang and L. Wang, *Journal of Alloys and Compounds*, **857**, 158112(2021), https://doi.org/10.1016/j.jallcom.2020.158112
10. Q. Zhao, Y. Chen, Y. Xu, R. Torrens, L. Bolzoni and F. Yang, *Materials & Design*, **200**, 109457(2021), https://doi.org/10.1016/j.apt.2021.05.009
11. S. Dong, G. Ma, P. Lei, T. Cheng, D. Savvakin and O. Ivasishin, *Advanced Powder Technology*, **58**, 921(2021), https://doi.org/10.1016/j.apt.2021.05.009
12. Y. Zhang, S. Fang, Y. Wang and D. Zhang, *Materials Science and Engineering: A*, **803**, 140701(2021), https://doi.org/10.1016/j.msea.2020.140701
13. Y. Liu, Z. Liu and M. Wang, *Journal of Materials Processing Technology*, **294**, 117142(2021), https://doi.org/10.1016/j.jmatprotec.2021.117142
14. J. Bautista-Ruiz, J.C. Caicedo and A. Chaparro, *Rasayan Journal of Chemistry*, **12(4)**, 1950(2019), https://doi.org/10.31788/RJC.2019.1245390
15. B. Shahabi Kargar, M.H. Moayed, A. Babakhani, A. Davoodi, *Corrosion Science*, **53(1)**, 135(2011), https://doi.org/10.1016/j.corsci.2010.09.004

16. P. Murkute, S. Pasebani and O. Burkan-Isgor, *Journal of Materials Processing Technology*, **273**, 116243(2019), https://doi.org/10.1016/j.jmatprotec.2019.05.024
17. J.E. Sanchéz, L. Ipaz, W. Aperador, J.C. Caicedo, C. Amaya, M.A.H Landaverde, F.E Beltran, J. Muñoz-Saldaña and G. Zambrano, *Applied Surface Science*, **256(8)**, 2380(2010), https://doi.org/10.1016/j.apsusc.2009.10.071
18. T. Meesak and C. Thedsuwan, *Materials Today: Proceedings*, **5(3)**, 9560(2018), https://doi.org/10.1016/j.matpr.2017.10.138
19. J. Bautista-Ruiz, G. Moreno and A. Chaparro, *Rasayan Journal of Chemistry*, **13(3)**, 1711(2020), https://doi:10.31788/RJC.2020.1335521
20. L. Romero-Resendiz, P. Gómez-Sáez, A. Vicente-Escuder and V. Amigó-Borrás, *Journal of Materials Research and Technology*, **11**, 1719(2021), https://doi.org/10.1016/j.jmrt.2021.02.014
21. X. Song, F. Liu, C. Qiu, E. Coy, H. Liu, W. Aperador, K. Załęski, J. Li, W. Song, Z. Lu, H. Pan, L. Kong and G. Wang, *Materials Horizons*, **2021(8)**, 912(2021), https://doi.org/10.1039/D0MH01837F
22. M. Fellah, N. Hezil, M. Zine Touhami, M. AbdulSamad, A. Obrosov, D. O. Bokov, E. Marchenko, A. Montagne and A. Alhussein, *Journal of Materials Research and Technology*, **9(6)**, 14061(2020), https://doi.org/10.1016/j.jmrt.2020.09.118
23. J. Chávez, O. Jimenez, L. Olmos, I. Farias, M. Flores-Jimenez, R. Suárez-Martínez, J.L. Cabezas-Villa and J. Lemus-Ruiz, *Materials Letters*, **280**, 128590(2020), https://doi.org/10.1016/j.matlet.2020.128590
24. M. Belwanshi, P. Jayaswal and A. Aherwar, *Materials Today: Proceedings,* **44(6)**, 4131(2021), https://doi.org/10.1016/j.matpr.2020.10.458
25. J. Bautista-Ruiz, W. Aperador and M.R. Joya, *Rasayan Journal of Chemistry,* **13(4)**, 2092(2020), https://doi:10.31788/RJC.2020.1345854

[RJC-6622/2021]